Electromagnetic waves emitted from an electron-positron plasma cloud moving across a magnetic field

Tadashi Kitanishi,[1] Jun-Ichi Sakai,[1] Ken-Ichi Nishikawa,[2] and Jie Zhao[1]
[1]*Department of Electronics and Information, Toyama University, Toyama 930, Japan*
[2]*Department of Space Physics and Astronomy, Rice University, Houston, Texas 77251*
(Received 14 September 1995; revised manuscript received 22 January 1996)

We have investigated the dynamics of an electron-positron plasma cloud moving perpendicular to an ambient magnetic field in a vacuum and also with background plasmas using a three-dimensional electromagnetic particle code. Simulation results show that charge sheaths are formed at both sides of the cloud and a polarized electric field is created inside the cloud by the coherent motion of cloud particles. This polarized electric field leads to the $E\times B$ drift motion of the cloud, and some of the cloud particles expand along the magnetic field from the charge sheaths. Consequently, linearly polarized electromagnetic waves are excited from the cloud. It should be noted that the kinetic energy of clouds is transformed very efficiently into the emitted wave energy during about one cyclotron period. This mechanism may be responsible to the emission of strong electromagnetic waves observed in electron-positron plasmas. [S1063-651X(96)03806-8]

PACS number(s): 52.35.Hr, 52.65.−y

I. INTRODUCTION

Plasma clouds and streaming plasmas in an ambient magnetic field are often found in many areas, ranging from astrophysical to laboratory plasmas. The cloud dynamics was investigated theoretically [1,2] and also by particle simulations [3–7]. Previous simulations were achieved for electron-ion plasmas using one-dimensional [3] and two-dimensional [4–6] electrostatic codes. Galvez [3] studied also electron-positron plasmas. Neubert *et al.* [7] investigated the dynamics of electron-ion plasma cloud using a three-dimensional electromagnetic, relativistic particle code.

Electron-positron plasmas have been extensively investigated; in laboratory [8,9], collective modes in nonrelativistic plasma [10,11], and astrophysical plasmas, for example, shock acceleration [12], magnetic reconnection [13,14], nonlinear wave propagation [15], current loop coalescence [16], and electron-beam dynamics [17,18]. Recently, an electron-positron annihilation line was observed around black hole candidates [19–21] and galactic centers [22], which imply a possibility that electron-positron plasmas could exist around these objects.

In this paper, we investigate the dynamics of an electron-positron cloud moving perpendicular to an ambient magnetic field and an associated emission of electromagnetic waves in a vacuum as well as in a background plasma using a three-dimensional electromagnetic and relativistic particle code [23,24]. We have found that the cloud keeps moving at the $E\times B$ drift motion due to the polarized electric field created by the charge sheaths which are formed at the both sides of the cloud. At the same time, some of the cloud particles expand along the magnetic field from the charge sheaths. Consequently, linearly polarized electromagnetic waves are excited from the cloud due to the coherent gyration of cloud particles, and the kinetic energy of cloud is transformed very efficiently into the emitted wave energy during about one cyclotron period.

This paper is organized as following. In Sec. II, we present the simulation model and parameters used in the simulation. In Sec. III we present the simulation results. We summarize our results and discuss some applications in Sec. IV.

II. SIMULATION MODEL AND PARAMETERS

We use the three-dimensional, fully electromagnetic and relativistic particle-in-cell (PIC) code developed by Buneman [24]. The system size used for the simulations is $L_x=L_y=70\Delta$, and $L_z=520\Delta$, where L_x, L_y, and L_z are the lengths of the system in three dimensions and $\Delta(=1)$ is the grid unit. Periodic boundary conditions are used for particles and fields in the z direction, while the radiating boundary conditions [25] are used in the x and y directions. Particles which hit these boundaries are arrested there and then 20% of them are randomly reflected with a thermal velocity. The size of the electron-positron plasma cloud is $L_{cx}=L_{cy}=L_{cz}=20\Delta$, where L_{cx}, L_{cy}, and L_{cz} are the cloud lengths in the x, y, and z directions, respectively. We use the cloud number density, $n^c=4$, which is four times larger than the background plasmas number density, $n^b=1$. The ambient magnetic field is homogeneous and in the z direction. The thermal velocity of particles is $v_{th}=0.04c$ and the initial drift velocity along the x direction is $V_0=0.3c$, where c $(=0.5)$ is the light velocity. The gyroradius of the cloud particles relate to V_0 is $r^c=2.0\Delta$. The ratio of the cyclotron frequency, Ω_e, to the plasma frequency in the cloud, ω_p^c, sets to $\Omega_e/\omega_p^c=1.5$. The Alfvén velocity defined in an electron-positron plasma as

$$v_A/c=\{1+2(\Omega_e/\omega_p)^2\}^{-1/2}, \tag{1}$$

is $v_A=0.905c$ in the background plasma. Other parameters are as follows: $m_p/m_e=1$, $\lambda_D=0.4\Delta$, $c/\omega_p^c=10.0\Delta$, $\omega_p\Delta t=0.025$, $T_c=83.7$ time steps, and $\beta=0.103$, where m_e, m_p, λ_D, c/ω_p^c, T_c, and β are the mass of electron, the mass of positron, (electron) Debye length in the cloud, skin

depth in the cloud, electron cyclotron period, and plasma beta in the cloud, respectively.

The reason why spatial resolution of only gyroradius is adequate is that all spatial scales are much larger than the gyroradius of the cloud particles relate to the initial cloud velocity, as we shall see below. Time step to get precise cyclotron motion is restricted by $\tan(\Omega_e \Delta t) \approx \Omega_e \Delta t < 0.2$ [24]. In this paper, $\Omega_e \Delta t = 0.075$, which satisfies the above restriction.

III. SIMULATION RESULTS

A. Sheath formation and expansion

We performed several cases in a vacuum and in background plasmas. Figure 1 shows the charge density and electric field on the x-y plane ($z = 260\Delta$) at $t = 0.5\omega_p^{-1}$ in a vacuum. The black and white shades show negative and positive charges, respectively. The arrows indicate the direction and strength of the electric field in the plane. The ambient magnetic field is pointing out of the plane, and the cloud moves due to this electric field toward the higher x value. When the cloud moves to the higher x value across the ambient magnetic field, the cloud positrons begin to rotate clockwise and the cloud electrons rotate counterclockwise (looked from the positive z direction). As a result, as shown in Fig. 1, a positive charge sheath, like a flat plane, is formed on the lower side of the cloud (at $y = 25\Delta$) and a negative charge sheath on the upper side (at $y = 45\Delta$). Consequently,

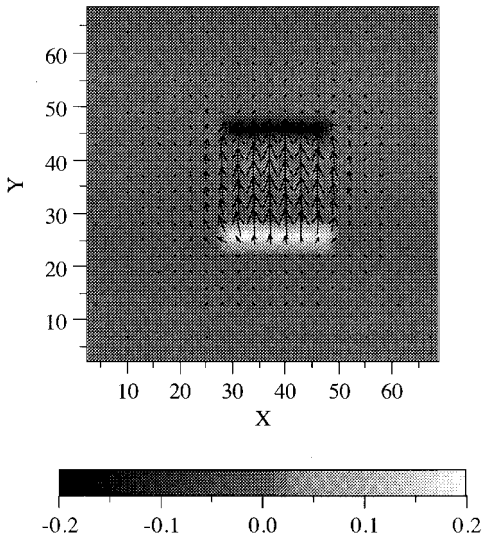

FIG. 1. The charge density and electric field on the x-y plane ($z = 260\Delta$) at $t = 0.5\omega_p^{-1}$ in a vacuum. The shades show the charge density. The arrows indicate the direction and strength of electric field in that plane.

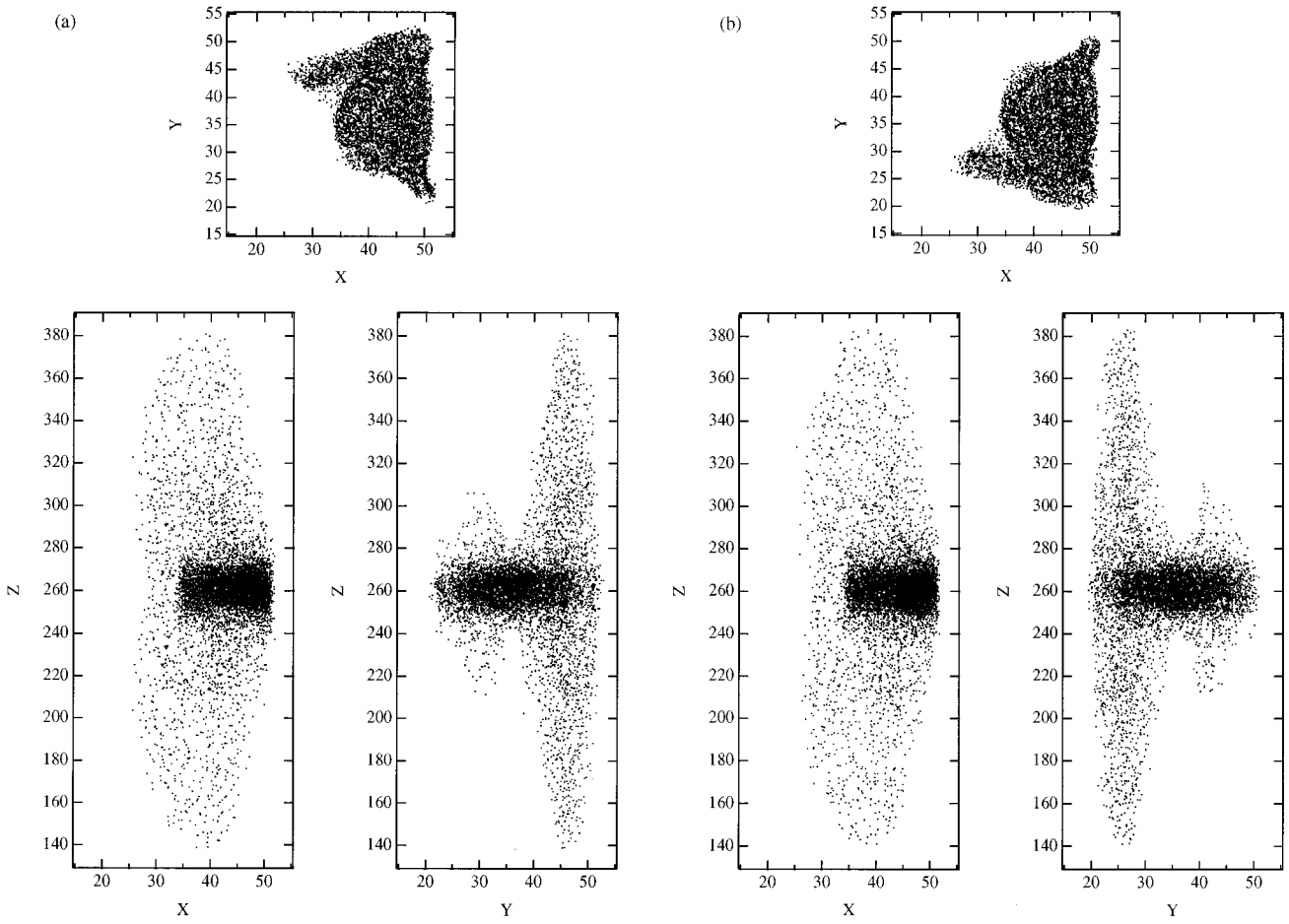

FIG. 2. The distribution of the cloud particles projected onto the x-y (top), x-z (bottom left), and y-z (bottom right) planes at $t = 12.5\omega_p^{-1}$ in a vacuum, (a) the cloud electrons, and (b) the cloud positrons.

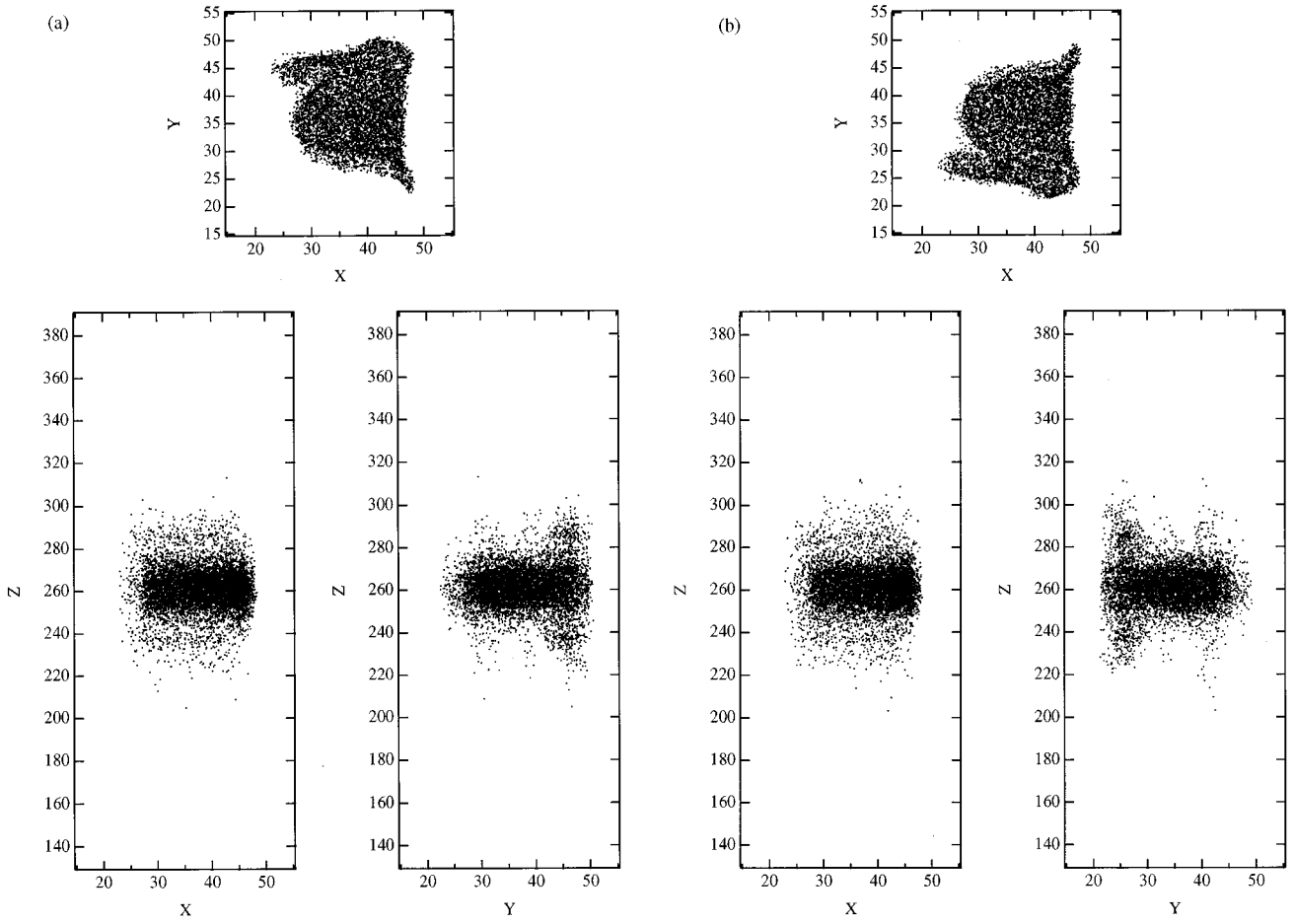

FIG. 3. The distribution of the cloud particles projected onto the x-y (top), x-z (bottom left), and y-z (bottom right) planes at $t=12.5\omega_p^{-1}$ in the background plasmas, (a) the cloud electrons, and (b) the cloud positrons.

these charge sheaths create a polarized electric field, E_p, inside the cloud in the y direction, which pushes the whole cloud by the $E_p \times B$ drift motion.

The space distributions of cloud particles are shown in the x-y (top frame), x-z (bottom left frame), and y-z (bottom right frame) planes at $t=12.5\omega_p^{-1}$ for the case in a vacuum in Fig. 2 [(a) the cloud electrons and (b) the cloud positrons]. As seen in the top panels, the cloud moves toward the higher x value. At the same time the cloud spreads at the head due to the compression of the magnetic field at the head of the cloud. It is also shown that the charge sheaths peel off at the tail of the cloud. The expansion of the charge sheaths along the magnetic field is shown in the bottom frames. As shown in the bottom right frames, some of the cloud particles expand along the magnetic field from the both charge sheaths. For example, as shown in Fig. 2(a), the electrons pile up around $y=45\Delta$, which creates the negatively charged sheath. Consequently, some electrons are expelled from this sheath. On the other hand, the positrons are expelled more strongly from the other sheath ($y=25\Delta$), as shown in Fig. 2(b). The expanding velocity along the magnetic field becomes faster if the ambient magnetic field is weaker or the initial drift velocity is faster. This is because that the charge sheaths grow widely or quickly due to the large gyroradius of the cloud particles. In this simulation, the particles are accelerated up to about a half of the light velocity at $t=12.5\omega_p^{-1}$.

The dynamics of the cloud is affected by background plasmas. Figure 3 shows the space distributions of the cloud particles projected onto the x-y (top frame), x-z (bottom left frame), and y-z (bottom right frame) planes at $t=12.5\omega_p^{-1}$ for the simulation with the background plasma. Figures 3(a) and 3(b) show the cloud electrons and positrons, respectively. All effects observed in a vacuum are also seen with the background plasmas. However, the charge sheaths are less developed and the particles are less accelerated than in a vacuum, since the background particles reduce the charge density in the charge sheaths.

B. Time history of the cloud velocity

In order to investigate the global evolution of the cloud, the time histories of the average cloud velocity in the x direction, V_x/V_0, are shown in Fig. 4. The solid and dashed curves show the cases in a vacuum and in the background plasmas, respectively.

In a vacuum case, the oscillation of the cloud velocity dumps within $1.5T_c$, and the cloud moves slowly toward the positive x value and its velocity decreases in time. The oscillation of the cloud velocity is related to a magnitude of the ambient magnetic field. When the ambient magnetic field is

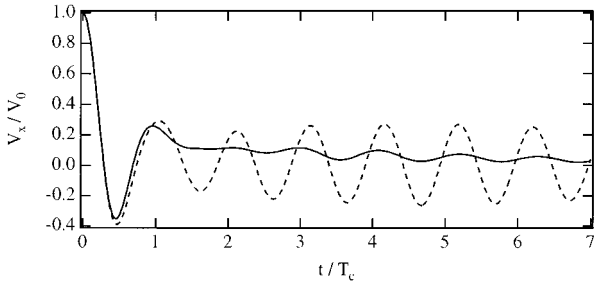

FIG. 4. Time evolutions of the mean cloud velocity (V_x) in the x direction are plotted by the solid curve for a vacuum, and by the dashed line for in the background plasmas. Velocities are normalized by the initial drift velocity (V_0).

strong (i.e., $\Omega_e/\omega_p^c \geqslant 2$), the cloud velocity keeps the oscillation with the cyclotron period and the amplitude of the oscillation decreases slowly with the small drift across the ambient magnetic field. While, if the ambient magnetic field is weak ($\Omega_e/\omega_p^c \leqslant 1$), the oscillation of the cloud velocity dumps quickly and after that, the cloud keeps moving.

In the background plasma case, as shown in Fig. 4, after the initial damping the cloud velocity keeps an undumped oscillation with the very small drift across the ambient magnetic field.

C. Waves emitted from the cloud

Due to the undumped oscillation of the cloud the strong waves are excited from the cloud. The time histories of the magnetic field B_x along the z direction ($130 \leqslant z \leqslant 390\Delta$) at $x=y=35\Delta$ are shown in Fig. 5 [(a) in a vacuum, and (b) in the background plasma]. Both figures indicate that electromagnetic waves with nearly the cyclotron frequency are generated and propagate away from the cloud. The oscillation of the polarized electric field due to the coherent gyromotion of the cloud particles is responsible for the generation of the electromagnetic waves. In a vacuum, the electromagnetic waves are generated strongly in the initial phase, but dump quickly. On the other hand, in the background plasma, the radiation last longer due to the undumped oscillation of the cloud, as shown in Fig. 4.

Figure 6 shows the hologram of the magnetic field amplitude (B_x, B_y) in the x-y plane ($x=y=35\Delta, z=320\Delta$) in the background plasmas. As shown in Fig. 6, the amplitude of B_y is much less than that of B_x ($\approx B_x/50$). Therefore, we find that the excited wave is linearly polarized with the B_x component. This comes from the fact that E_y is created dominantly inside the cloud and oscillates due to the coherent gyration of cloud particles.

The dispersion relations of the wave B_x shown in Fig. 5 are shown in Fig. 7 [(a) in a vacuum, and (b) in the background plasma]. The wave intensities are obtained performing a two-dimensional Fourier transform (one-space and one-time) for the first 512 time steps. In a vacuum, the electromagnetic waves with around Ω_e is excited on the dispersion relation of the light wave, as shown in Fig. 7(a). Another large amplitude wave with around $\omega=\Omega_e$ and large k_z corresponds to the upper hybrid wave propagating obliquely to the ambient magnetic field with the cloud moving.

For the waves propagating parallel to the magnetic field in

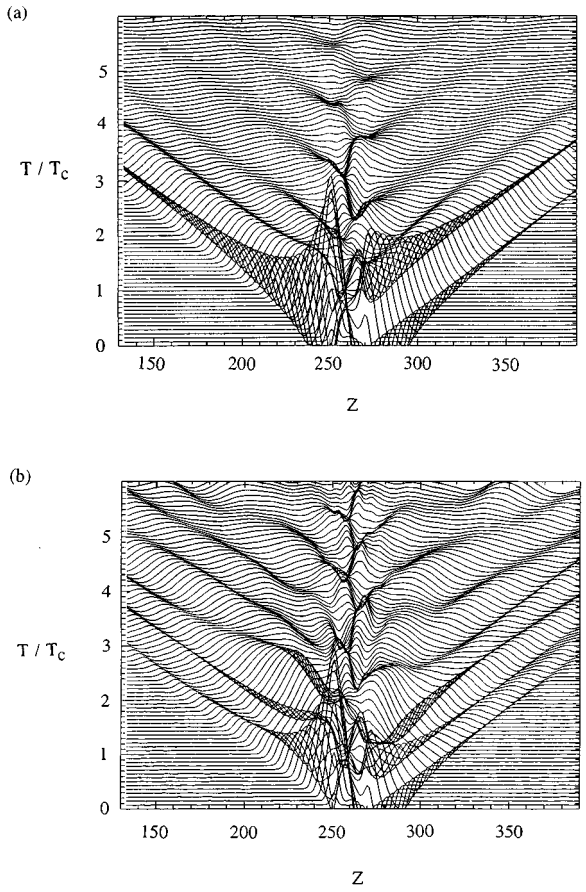

FIG. 5. Time evolution of B_x along the z direction ($130\Delta \leqslant z \leqslant 390\Delta$) in the center of the x-y plane ($x=y=35\Delta$); (a) in a vacuum, and (b) in the background plasmas.

electron-positron plasmas, as noted in Refs. [10,11], the left and right circularly polarized waves have the same dispersion and a whistler mode does not exist. The dispersion relation of the waves parallel to the magnetic field is [10,11]

$$2\omega_{\pm}^2 = c^2k^2 + 2\omega_p^2 + \Omega_e^2 \pm \sqrt{(c^2k^2 + 2\omega_p^2 - \Omega_e^2)^2 + 8\omega_p^2\Omega_e^2}, \tag{2}$$

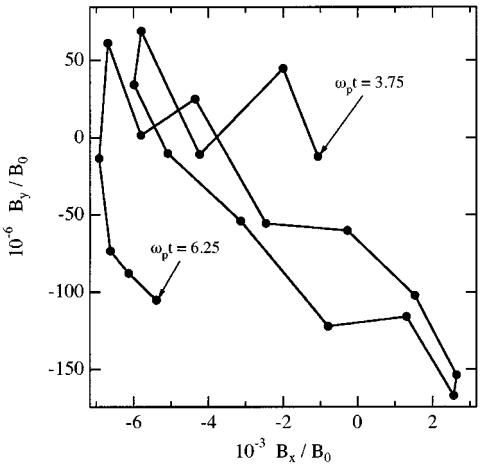

FIG. 6. Time history of B_x vs B_y from $t=3.75\omega_p^{-1}$ (150 time steps) to $6.25\omega_p^{-1}$ (250 time steps) taken at $x=y=35\Delta$, $z=320\Delta$. Each value is plotted every 5 time steps. B_x and B_y are normalized to the ambient magnetic field, B_0.

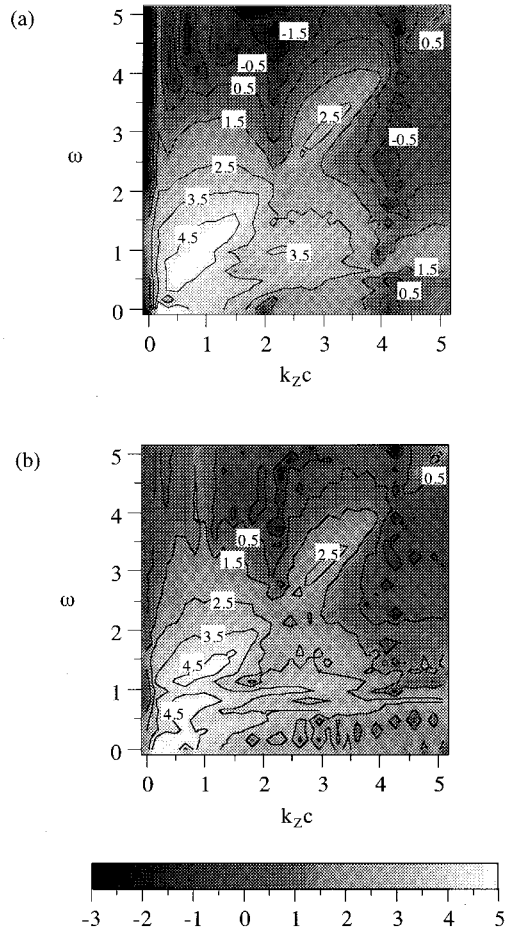

FIG. 7. Wave intensity of B_x as a function of ω and k_z corresponding to Fig. 5. ω and k_z are normalized to Ω_e and Ω_e/c, respectively. (a) in vacuum, and (b) in the background plasma.

where ω_+ and ω_- correspond to the electromagnetic mode and the Alfvén mode, respectively. On the other hand, in the background plasmas, there are two branches which correspond to $\omega_\pm$ in Fig. 7(b).

D. Energy conversion

The time evolution of the energy in the simulation system, whose size is changed to $136\Delta \times 136\Delta \times 136\Delta$ in a vacuum, is shown in Fig. 8. Up to $t = 1.4T_c$, the front of the waves emitted from the cloud does not reach to any boundary; therefore the total energy in this simulation system is conserved. Solid and dashed curves show the kinetic energy of the cloud and the field energy in the simulation system, respectively. As shown in Fig. 8, nearly 80% of the initial kinetic energy of the cloud is converted to the field energy during $1T_c$. With background plasmas, the conversion rate from initial kinetic energy of the cloud to field energy within $1T_c$ is less than that in a vacuum, because the kinetic energy of the cloud is also converted to that of the background plasmas. Nevertheless, nearly 40% of the initial kinetic energy of the cloud is converted to the field energy.

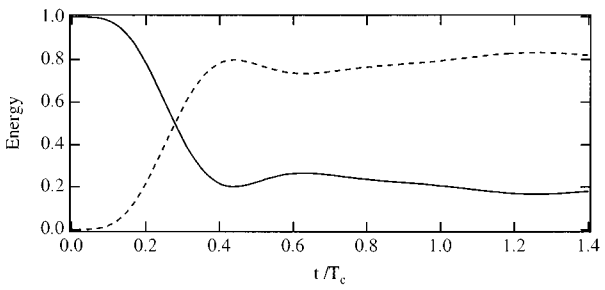

FIG. 8. Time evolution of the energies in the simulation system in a vacuum. A solid and dashed curves present the kinetic energy of the cloud and the field energy, respectively. Energies are normalized to the kinetic energy of the cloud at $t = 0$.

IV. SUMMARY AND APPLICATIONS

We have investigated the dynamics of the electron-positron plasma cloud moving perpendicular to the ambient magnetic field and the associated emission of electromagnetic waves from the cloud in a vacuum and the background plasma, using the three-dimensional electromagnetic particle code developed by Buneman [24]. The results of our simulation are as following. At first, by the coherent motion of the cloud perpendicular to the magnetic field, charge sheaths are formed at the both sides of the cloud and a polarized electric field, E_p, is created inside the cloud. Therefore, the cloud moves to the same direction as the initial drift velocity with $E_p \times B$ drift, at the same time cloud particles expand along the magnetic field from the charge sheaths. Associated with these motions, linearly polarized electromagnetic waves are excited from the cloud. In the simulations, it is also found that the kinetic energy of the cloud is efficiently converted to the emitted wave energy during $1T_c$. We note that for the coherent motion of the cloud perpendicular to the ambient magnetic field is responsible for the emission of electromagnetic waves.

These simulation results may be applicable to an emission mechanism of electromagnetic waves from the magnetospheres of black hole and the active galactic center. We propose a possible scenario. When a part of the edge of the inner accretion disk, which consists of electron-positron plasmas, happens to fall into a central object due to instabilities such as the Kelvin-Helmholtz instability and the Rayleigh-Taylor instability, the electron-positron plasma cloud gains its kinetic energy from the gravitational force of the central object, and then moves across the magnetic field produced by the central object. In such a circumstance the kinetic energy of the cloud can be effectively converted to the electromagnetic wave energy. Furthermore, a portion of the cloud particles escapes from the cloud along the magnetic field which may lead to a generation of beams.

ACKNOWLEDGMENTS

This work was supported by the U.S.-Japan cooperative science program of JSPS and by NSF (INT-9217650). K.-I.N. is supported by NSF under Grants No. ATM 9119814 and No. ATM 9121116. J.S. is partly supported by a Grant in Aid for Scientific Research from the Ministry of Education (07247208).

[1] W. Peter and N. Rostoker, Phys. Fluids **25**, 730 (1982).
[2] J. E. Borovsky, Phys. Fluids **30**, 2518 (1987).
[3] M. Galvez, Phys. Fluids **30**, 2729 (1987).
[4] M. Galvez, G. Gisler, and C. Barnes, Phys. Fluids B **1**, 2516 (1989).
[5] M. Galvez and J. E. Borovsky, Phys. Fluids B **3**, 1892 (1991).
[6] D. S. Cai and O. Buneman, Phys. Fluids B **4**, 1033 (1992).
[7] T. Neubert, R. H. Miller, O. Buneman, and K.-I. Nishikawa, J. Geophys. Res. **97**, 12 057 (1992).
[8] R. G. Greaves, M. D. Tinkle, and C. M. Surko, Phys. Plasmas **1**, 1439 (1994).
[9] R. G. Greaves and C. M. Surko, Phys. Rev. Lett. **75**, 3846 (1995).
[10] N. Iwamoto, Phys. Rev. E **47**, 295 (1992).
[11] G. P. Zank and R. G. Greaves, Phys. Rev. E **51**, 6079 (1995).
[12] M. Hoshino, J. Arons, Y. A. Gallant, and A. B. Langdon, Astrophys. J. **390**, 454 (1992).
[13] E. G. Blackman and G. B. Field, Phys. Rev. Lett. **71**, 3481 (1993).
[14] E. G. Blackman and G. B. Field, Phys. Rev. Lett. **72**, 494 (1994).
[15] T. Tajima and T. Taniuti, Phys. Rev. A **42**, 3587 (1990).
[16] J. Zhao, J. I. Sakai, and K. I. Nishikawa, Phys. Plasmas **3**, 844 (1996).
[17] J. Zhao, K. I. Nishikawa, J. I. Sakai, and T. Neubert, Phys. Plasmas **1**, 103 (1994).
[18] J. Zhao, J. I. Sakai, K. I. Nishikawa, and T. Neubert, Phys. Plasmas **1**, 4114 (1994).
[19] J. C. Ling and W. A. Wheaton, Astrophys. J. **343**, L57 (1989).
[20] A. Goldwurm *et al.*, Astrophys. J. **389**, L79 (1992).
[21] R. Sunyaev *et al.*, Astrophys. J. **389**, L75 (1992).
[22] L. Bouchet *et al.*, Astrophys. J. **383**, L45 (1991).
[23] K.-I. Nishikawa, O. Buneman, and T. Neubert, Geophys. Res. Lett. **21**, 1019 (1994).
[24] O. Buneman, in *Computer Space Plasma Physics, Simulation Techniques and Software*, edited by H. Matsumoto and Y. Omura (Terra Scientific, Tokyo, 1993), p. 67.
[25] E. L. Lindman, J. Comput. Phys. **18**, 66 (1975).